ELSEVIER

Synthesis and characterization of alkaline polyvinyl alcohol and poly(epichlorohydrin) blend polymer electrolytes and performance in electrochemical cells

Chun-Chen Yang[*], Sheng-Jen Lin, Sung-Ting Hsu

Department of Chemical Engineering, MingChi Institute of Technology, Taipei, Hsien 243, Taiwan, ROC

Abstract

Alkaline SPE was obtained from a blend of polyvinyl alcohol (PVA) and poly(epichlorohydrin) (PECH), PVA–PECH, by a solution-cast technique. The PVA host polymer is blended with PECH polymer to provide a polymer electrolyte with improved chemical and mechanical properties. The ionic conductivity of the PVA–PECH polymer electrolytes is between 10^{-2} and $10^{-3}\,S\,cm^{-1}$ at room temperature when the blend ratio is varied from 1:0.2 to 1:1. The PVA–PECH polymer was characterized by means of scanning electron microscopy, X-ray diffraction, stress–strain test, cyclic voltammetry, and a.c. impedance spectroscopy. It is found that the polymer electrolytes exhibit good mechanical strength and excellent chemical stability. The electrochemical performance of solid-state Zn–air batteries with various types of the blended polymer electrolyte films is examined by a galvanostatic discharge method.
© 2003 Elsevier Science B.V. All rights reserved.

Keywords: Alkaline polymer electrolyte; Polyvinyl alcohol; Poly(epichlorohydrin); Ionic conductivity; Zn–air battery

1. Introduction

Solid polymer electrolytes (SPEs) have been extensively studied in recent years for application in many electrochemical devices, such as cellular phones, smart credit cards, and laptop computers [1]. Polymer complexes of polyethylene oxide (PEO), plasticizers, and alkali metal salts were discovered by Wright and coworkers [2,3] and Armand et al. [4]. Although a PEO-based SPE can form a dimensionally stable film, its ambient temperature conductivity is in the range 10^{-7} to $10^{-8}\,S\,cm^{-1}$. This is too low for application in electrochemical devices. In order to enhance the conductivity, several approaches have been suggested. Blended polymer electrolytes [5–9], polymer electrolytes modified with a plasticizer or a mixture of solvents, and polymer electrolytes with micro or nano-sized ceramic filler particles [10–15] have been extensively explored. The main goal of these studies is to obtain films with a high fraction of amorphous phase, which exhibits a much higher conductivity than the crystalline phase.

Some studies have focused on PEO-based electrolytes with lithium salts and organic solvents. The polymer lithium system appears to be the most widely examined due to its potential application in batteries with high specific energies. There are few reports on alkaline SPEs systems [15–18]. Work in our laboratories has shown that alkaline polymer electrolyte [19] or alkaline composite polymer electrolyte [20,21] can be applied in alkaline Zn–air primary batteries and rechargeable Ni–MH batteries. In the present work, we report the preparation and properties of an alkaline SPE based on a polymer which is a blend of polyvinyl alcohol (PVA) and poly(epichlorohydrin) (PECH). A primary solid-state Zn–air batteries with PVA–PECH films is assembled and examined.

2. Experimental

PVA (MW 75,000–80,000, Chang-Chung Chemicals), PECH (MW 700,000, Aldrich), dimethy sulfoxide $(CH_3)_2SO$ (DMSO with an assay of 99.99%, Aldrich), and KOH (Merck) were used as received. The alkaline blended polymer electrolyte films were prepared by a solution-cast method. Appropriate weights of PVA were dissolved in DMSO with agitation at rotation of 1000 rpm for about 1 h at 60 °C. Suitable amounts of PECH were also dissolved in

* Corresponding author. Tel.: +886-2-2908-9899;
fax: +886-2-2904-1914.
E-mail address: ccyang@ccsun.mit.edu.tw (C.-C. Yang).

DMSO with agitation at 1000 rpm for about 5–7 h at 60 °C. After both the PVA and the PECH polymer were completely dissolved in DMSO, the resulting solutions were mixed together and stirred continuously until the solution took on a homogeneous, highly viscous appearance. The resulting homogeneous solutions were poured on to a petri dish and weighed immediately. The excess DMSO solvent was then evaporated slowly at 60 °C in a vacuum oven. After evaporation, the petri dish with the polymer film was re-weighed.

The polymer films were then dipped into 32 wt.% KOH solution for various periods. After immersion, the films were re-weighed. The chemical composition of the polymer films was calculated from the mass balance. The thickness of the films was controlled between 0.4 and 0.6 mm. The conductivity of the films was determined by means of the a.c. two-terminal method. The films were sandwiched between SS316 stainless-steel (SS), ion-blocking electrodes, each of surface area $0.785 \, cm^2$, in a spring-loaded glass holder. A thermocouple was located close to each film for temperature measurement. Cyclic voltammetry and a.c. impedance measurement were carried out with an EG&G impedance spectrometer model 273A+1025 and a computer program EG&G model 398. The frequency range from 300 kHz to 0.10 Hz at an excitation signal of 10 mV was recorded. A Hg | HgO electrode was used as a reference electrode. The impedance of the films was measured from 30 to 70 °C. Experimental temperature were maintained within ±0.2 °C by a convection oven.

The crystal structures of alkaline blended polymer electrolytes films were examined with a Philips X'Pert X-ray diffractrometer (XRD) with Cu Kα radiation of wavelength $\lambda = 1.54056 \, \text{Å}$ for 2θ angles between 10 and 80°. The water in the specimen was removed by freeze drying without any change in the morphology of the specimen. The surface morphology and microstructure of the film were characterized with a S-2600H scanning electron microscope (Hitachi Co., Ltd.). The mechanical strength of the films was measure by stress–strain test using an Instron model 5544 universal-testing instrument. The polymer electrolyte samples were kept in a plastic bag prior to the experiment.

The carbon slurry for the gas-diffusion layer was prepared with a mixture of 70 wt.% Shawinigan acetylene black (AB50) and 30 wt.% PTFE (teflon-30 suspension) as a binder. The slurry was coated on a Ni-foam current-collector, then pressed at a pressure of $100 \, \text{kg} \, cm^{-2}$. The gas-diffusion layer was first sintered for about 30 min at 300 °C. The active layer of the air electrode was then prepared by spraying a mixture of a 15 wt.% PTFE, 5–10 wt.% $KMnO_4$, 60 wt.% Vulcan XC-72R, and an appropriate amount of isopropyl alcohol on to the gas-diffusion layer. The air electrode with both the gas-diffusion layer and the active layer was finally sintered for about 30 min at 360 °C, under a pressure of $80 \, \text{kg} \, cm^{-2}$. The thickness of the air cathode electrode was between 0.4 and 0.6 mm. Zinc powder gels were prepared according to the following formulation: 67 wt.% Zn pow-

der, 1 wt.% Carbopol 940 gelling agent, 32 wt.% KOH, and some metal additives. Solid-state Zn–air cells, each with a PVA–PECH blended polymer electrolyte, an air electrode and a Zn gel anode, were assembled and examined. Cells with SPE films that had different ratios of PVA and PECH were discharged at the $C/10$ rate at 25 °C. Cells with the alkaline PVA–PECH (1:0.2) SPE were discharged at various C-rates at 25 °C. The bulk resistance (R_b) of each Zn–air cell was measured both before and after discharging by means of the a.c. impedance method. The electrochemical characteristics of the cells were evaluated with a BAT 778 model charge–discharge unit. The preparation method and measuring systems for Zn–air batteries have been reported in detail elsewhere [21].

3. Results and discussion

3.1. Surface morphology

A scanning electron micrograph of a blended polymer electrolyte film with a ratio of PVA:PECH of 1:0.2 is shown in Fig. 1. The film exhibits a uniform and homogeneous surface morphology. There is no phase-separation morphology and the films appear transparent. These alkaline polymer electrolytes form a free-standing film with good mechanical strength and good chemical stability. A micrograph of a PVA–PECH (1:0.5) SPE film is shown in Fig. 2. Some larger polymer aggregates or chunks are clearly discernible on the film. The micrograph also indicated that phase-separation of PVA and PECH becomes favorable. A PVA–PECH (1:1) SPE film exhibits phase-separated morphology, as shown in Fig. 3. A number of white particles of PVA are present in the film. Immiscibility of PVA with PECH at a high blend ratio is also observed.

3.2. Structural analysis of blended polymer films

The crystallinity of the blended polymer films was examined by means of XRD. Diffraction patterns for pure PVA powder and PVA–PECH films are presented in Fig. 4. The data show that the PVA polymer has a semi-crystalline structure with peak at a 2θ angle of 20°. As PECH is added, the intensity of the PVA peaks is greatly reduced. This implies that the addition of PECH into a PVA host increases the amorphous region. As seen in Fig. 4, the patterns for the PVA–PECH films have a broad peak, i.e. an 'amorphous hump.' This indicates that the film is an amorphous polymer material. The degree of amorphous character increases with increasing the PVA:PECH ratio. The mechanism of ionic transport in polymer electrolytes is still not clear, but there is significant transport in a polymer chain which has an amorphous phase, while a crystalline phase is non-conducting. The amorphous character produces greater ionic conductivity due to local structural relaxation and segmental motions in the polymer.

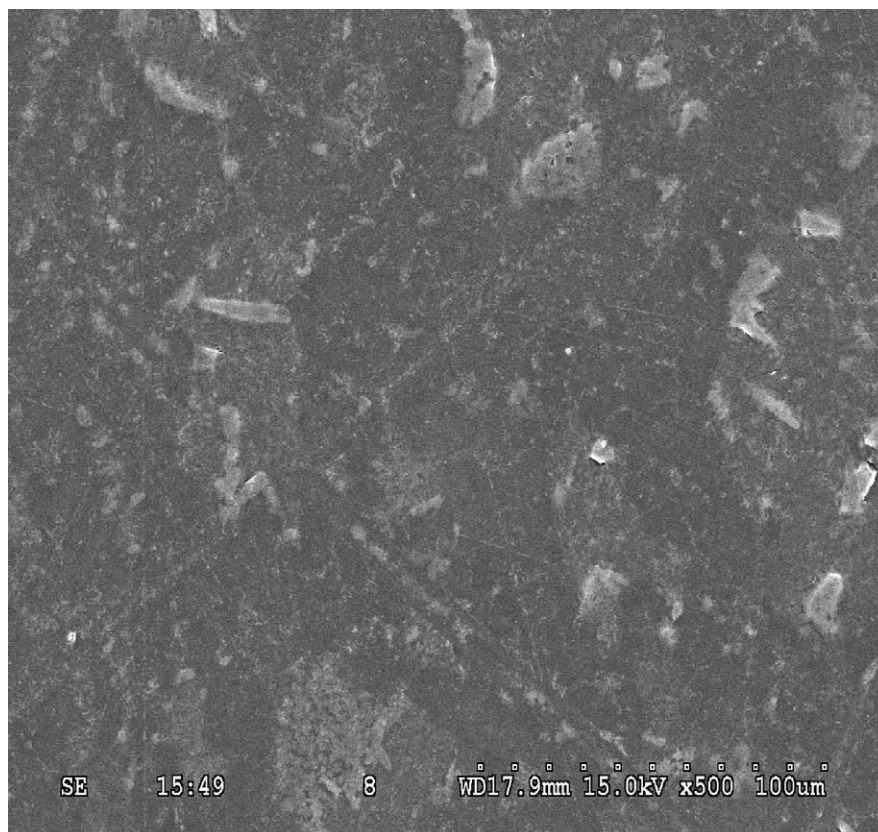Fig. 1. Scanning electron micrograph of alkaline PVA–PECH (1:0.2) SPE.

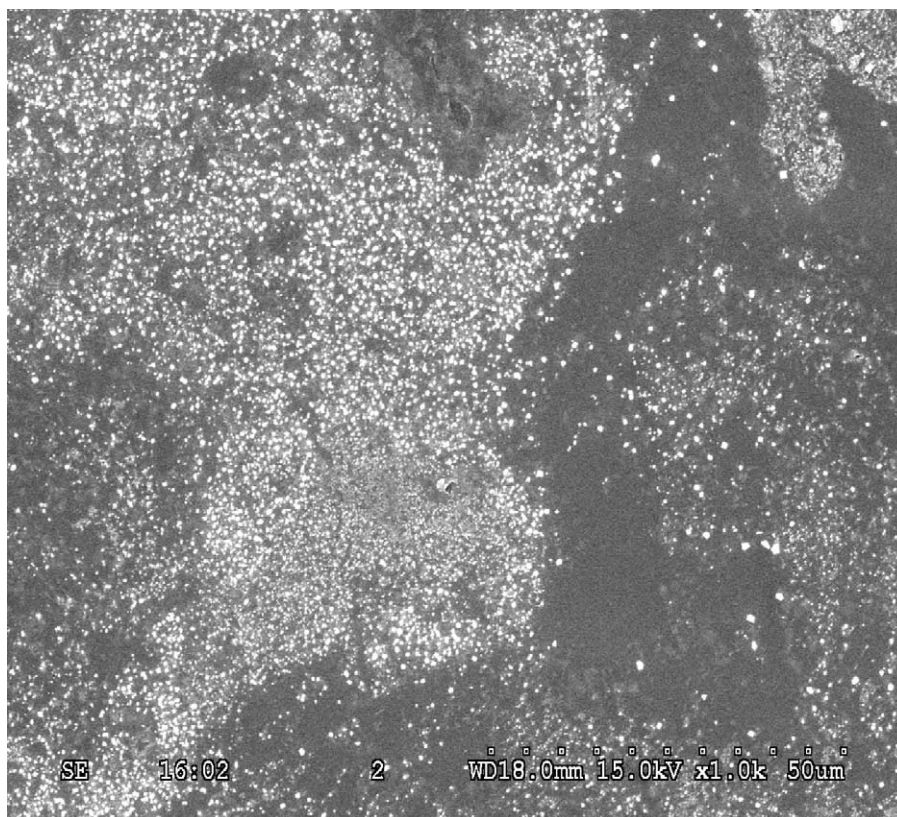Fig. 2. Scanning electron micrograph of alkaline PVA–PECH (1:0.5) SPE.

Fig. 3. Scanning electron micrograph of alkaline PVA–PECH (1:1) SPE.

3.3. Conductivity measurements of PVA–PECH polymer electrolyte films

The a.c. impedance spectra for PVA–PECH (1:0.2) polymer electrolytes are given in Fig. 5. The spectra were obtained from a SS|PVA–PECH–KOH SPE|SS cell and display two well-defined regions: (a) a high frequency range, which is related to the ionic conduction process in the bulk of the polymer electrolytes; (b) a low frequency range, with a straight line parallel to the imaginary
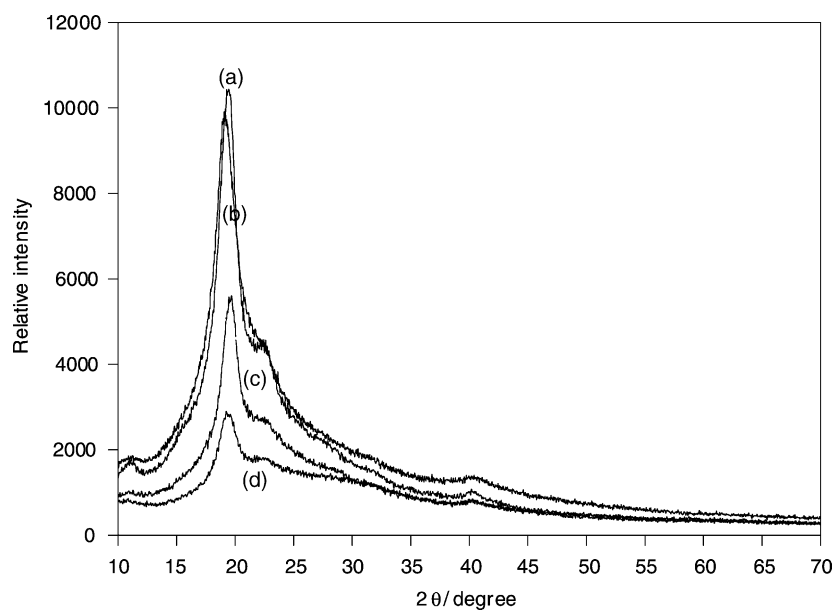

Fig. 4. XRD spectra for alkaline PVA–PECH SPE films: (a) pure PVA; (b) PVA:PECH = 1:0.2; (c) PVA:PECH = 1:0.5; and (d) PVA:PECH = 1:1.
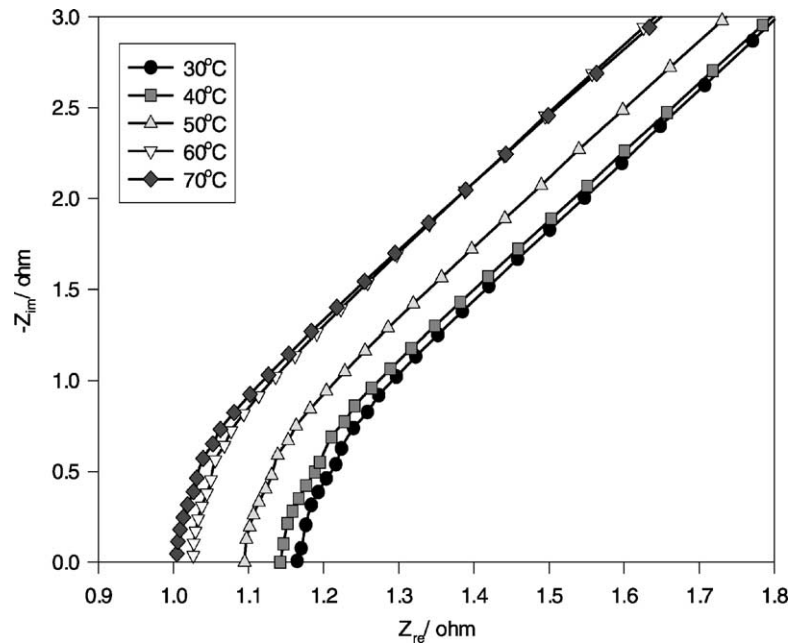
Fig. 5. a.c. impedance for alkaline PVA–PECH (1:0.2) polymer electrolyte films at various temperatures.

axis that is attributed to the effect of blocking electrode.

Since a blocking electrode was used in impedance analyses, the film | electrode interface can be regarded as a capacitance. When the capacitance is ideal, it should show a vertical spike in the impedance spectrum (Nyquist plot). In fact, a spike inclined at an angle of less than 90° is found instead of a vertical spike. This is known to be due to the roughness of the film | electrode interface.

Analysis of the spectra yields information about the properties of the electrolyte, such as the bulk resistance, R_b. This resistance can be calculated from the intercept at the higher frequency side on the Z_{re} axis. The R_b value can be converted to the ionic conductivity of the polymer electrolyte, σ, by means of the relationship $\sigma = l/R_b A$, where l is the thickness (cm) of the PVA–PECH blend polymer film, A is the area of the blocking electrode (cm^2), and R_b is the bulk resistance (Ω).

Typically, the R_b values for the alkaline PVA–PECH polymer electrolytes are of the order of 1–5 Ω and are dependent on the amount of KOH solution in the film. The ionic conductivities are in the order of 10^{-2} to 10^{-3} S cm^{-1}, as shown in Table 1. It is notable that the ionic conductivity

of an alkaline PVA–PECH (1:0.2) polymer electrolytes is higher than that of electrolytes with blend ratios of 1:0.5 and 1:1.

3.4. Effect of immersion time and temperature on ionic conductivity of SPE

The variation of KOH content versus immersion time for various blended PVA–PECH SPE films at 25 °C is presented in Fig. 6. The KOH content in the polymer films reaches a constant value after immersion for 70 h. The polymer with a blend ratio of 1:1 exhibits the lowest KOH content, but the lowest ionic conductivity at room temperature. This may be due to phase-separation of the PVA–PECH blended polymer films (immiscibility). The variation in ionic conductivity with immersion time for the different polymer electrolyte films is given in Fig. 7. In general, the higher the KOH content, the higher is the ionic conductivity.

The temperature dependence of the ionic conductivity of PVA–PECH films follows the Arrhenius relationship; $\log_{10}(\sigma)$ versus $1/T$ plots, as shown in Fig. 8, give the activation energy, E_a, which is dependent on the content of both

Table 1
Conductivity (S cm^{-1}) of alkaline PVA–PECH blended polymer electrolytes with various blend ratios at different temperatures

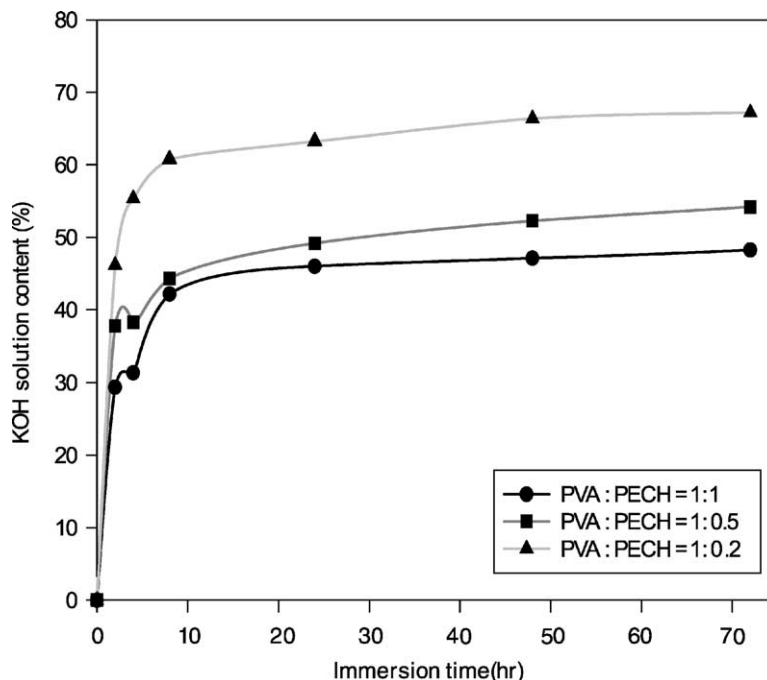| Temperature (°C)	PVA	PVA:PECH (1:0.2)	PVA:PECH (1:0.5)	PVA:PECH (1:1)
30	0.0471	0.0219	0.00459	0.0012
40	0.0499	0.0233	0.00462	–
50	0.0528	0.0238	0.00469	–
60	0.0560	0.0248	0.00480	–
70	0.0570	0.0254	0.00497	–

Fig. 6. Effect of immersion time on KOH content in PVA–PECH SPE films with different blend ratios at 25 °C.

KOH and water in the film. The values of E_a are in the range of 1–3 kJ/mol, i.e. less than those of alkaline PVA–KOH polymer electrolyte films (3–15 kJ/mol) [21].

3.5. Cyclic voltammetry of alkaline blended polymer electrolyte films

High conductivity is not sufficient to make the polymer electrolyte suitable for practical battery applications. In cyclic voltammetric studies, the potential was first scanned in the negative-going direction and then reversed. A broad electrochemical stability window is important for the practical use of these films. Cyclic sweeping between −1.5 and +1.5 V of a SS | SPE | SS cell is shown in Fig. 9. The stability of the electrolyte at the interface with the SS electrode is limited by a potential of about +1.0 V on the anodic side and −1.0 V on the cathodic side, which gives a window of about 2.0 V.
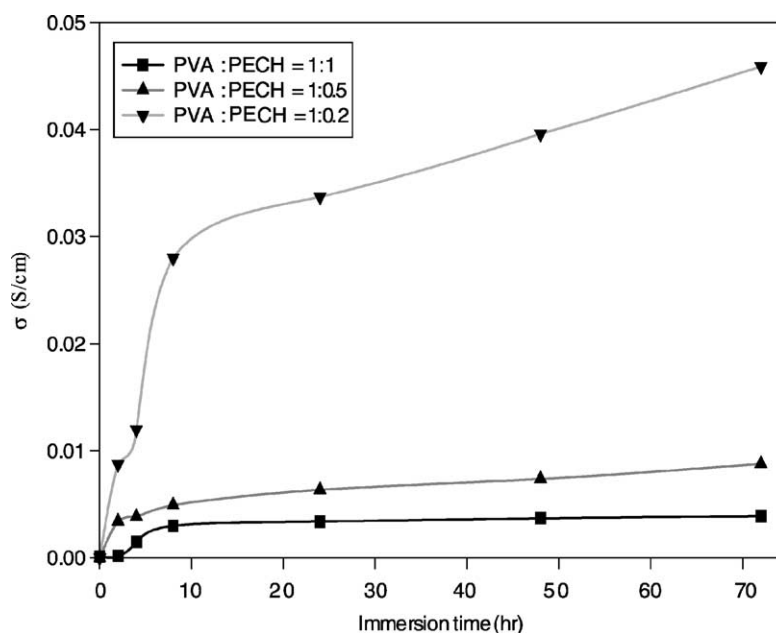

Fig. 7. Effect of immersion time on ionic conductivity of alkaline PVA–PECH SPE films with different blend ratios at 25 °C.
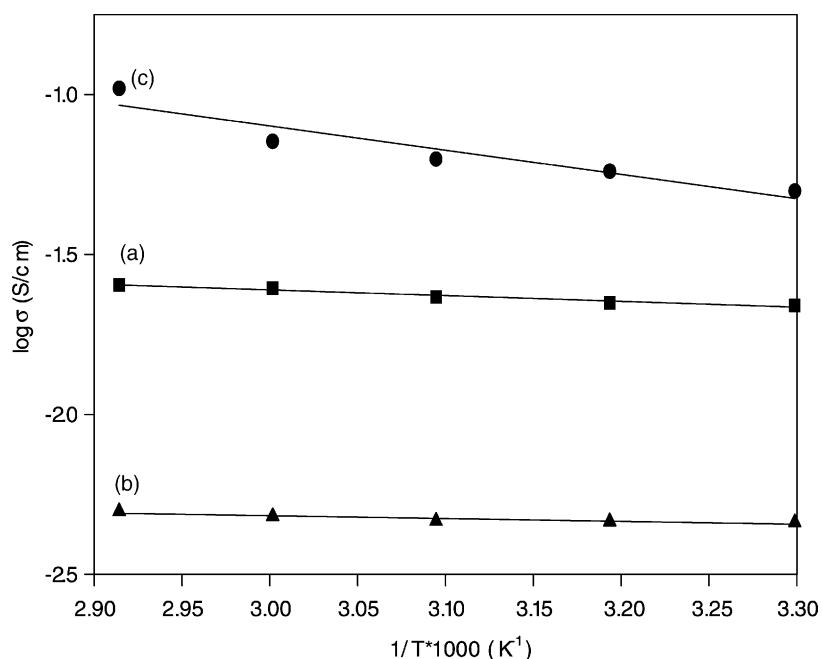
Fig. 8. Arrhenius plot for alkaline PVA–PECH polymer electrolytes with different blend ratios: (a) PVA:PECH = 1:0.2; (b) PVA:PECH = 1:0.5; and (c) PVA:PECH = 1:1.
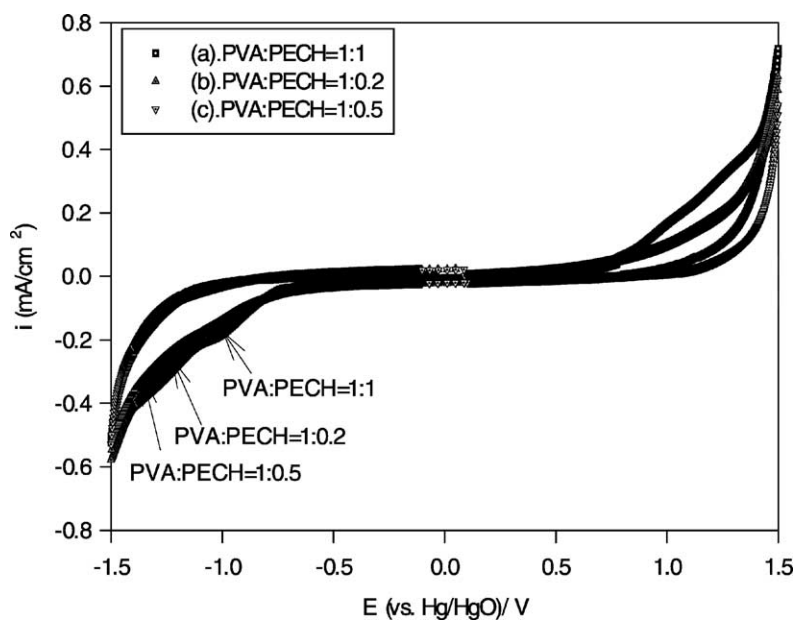

Fig. 9. Cyclic voltammograms for the alkaline PVA–PECH SPE films with various blend ratios at 25 °C, scan rate 1 mV s^{-1}.

Table 2
Mechanical strength of PVA–PECH blended polymer electrolytes and separators at a pull rate of 200 mm min^{-1}

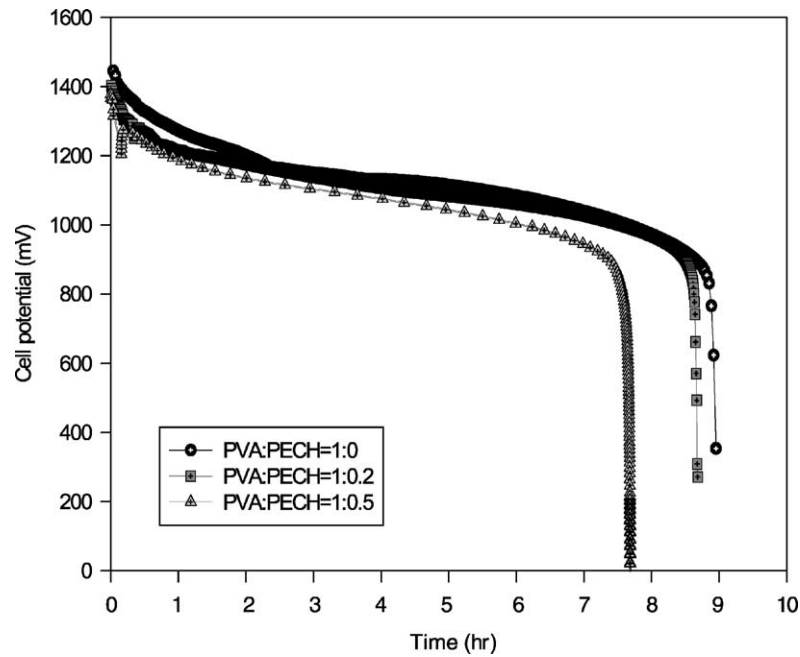| Film	Item				
	Thickness (mm)	Width (mm)	Strength (kg)	Stress (kg cm^{-2})	Elongation (%)
PVA–PECH (1:0)	0.16	10	0.6	37.5	457
PVA–PECH (1:0.5)	0.09	10	5.3	589	303
PVA–PECH (1:1)	0.13	10	3.4	262	106
Celguard separator	0.085	10	3.8	448	52
Gore PTFE separator	0.009	10	2.1	2378	58

Fig. 10. Discharge curve for Zn–air cell with different alkaline PVA–PECH polymer electrolyte films at 25 °C at *C*/10 rate.

3.6. Mechanical strength

The results of stress–strain tests of different types of alkaline blended polymer electrolytes and separators are shown in Table 2. An alkaline PVA–KOH film has a low yield stress viz., 37.5 kg cm^{-2}, but good elasticity with an elongation-at-break of 457%. By contrast, the alkaline PVA–PECH (1:0.5) film exhibits a yield stress of 589 kg cm^{-2}, with a low elongation-at-break of 303%. The higher the PECH content in the SPE, the lower is the me-

chanical strength of the polymer. By contrast, the yield stress of Celguard and Gore PTFE separators is 448 and 2378 kg cm^{-2}, respectively, as shown in Table 2.

3.7. Electrochemical performance of solid-state Zn–air battery

Discharge curves of Zn–air cells with different ratios of PVA–PECH polymer electrolytes at the *C*/10 discharge rate at 25 °C are shown in Fig. 10. The cell with a PVA–KOH
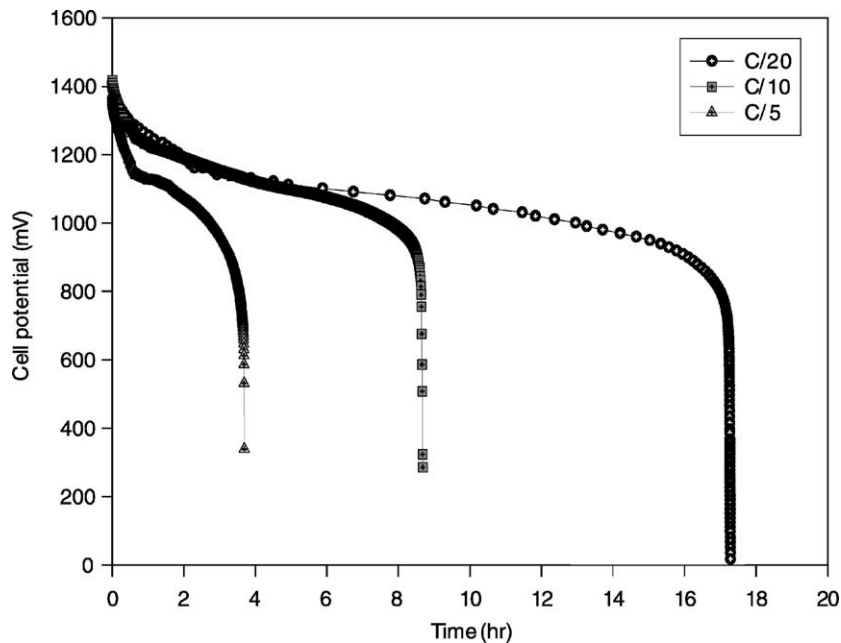

Fig. 11. Discharge curve for Zn–air cell with alkaline PVA–PECH (1:0.2) polymer electrolyte films at various discharge rates at 25 °C.

Table 3

Performance of solid-state Zn–air cells with different of PVA–PECH polymer films at $C/10$ rate

Parameter	PVA	PVA–PECH (1:0.2)	PVA–PECH (1:0.5)
Theoretical capacity (mAh)	1476	1476	1476
Discharge current (mA)	150	150	150
Discharge time (h)	8.92	8.60	7.73
Real capacity (mAh)	1338	1290	1160
Utilization (%)	89.0	86.1	77.0

Cell dimensions: $2\,cm \times 3\,cm$, area $= 6\,cm^2$.

Table 4

Performance of solid-state Zn–air cells with PVA–PECH (1:0.2) SPE at various discharge rates at $25\,°C$

Parameter	Discharge rate		
	$C/5$	$C/10$	$C/20$
Theoretical capacity (mAh)	1476	1476	1476
Discharge current (mA)	300	150	75
Discharge time (h)	3.69	8.59	17.28
Real capacity (mAh)	1107	1289	1296
Utilization (%)	73.8	85.9	86.4

Cell dimensions: $2\,cm \times 3\,cm$, area $= 6\,cm^2$.

polymer electrolyte exhibits the highest capacity (89% utilization), as shown in Table 3. By contrast, the utilization for cells with the PVA–PECH electrolytes at ratios of 1:0.2 and 1:0.5 are 86 and 77%, respectively. Discharge curves for the cells with PVA–PECH polymer electrolytes at various discharge rates are given in Fig. 11. The utilization of zinc material is in the range of 73–86% for rates of $C/5$–$C/20$, as shown in Table 4. The bulk resistance (R_b) of the cells was between 0.3 and 0.4 Ω before discharge, but greatly increased from 5 to 7 Ω after discharge.

4. Conclusions

Alkaline PVA–PECH blended polymer electrolytes with conductivites of the order of 10^{-2}–$10^{-3}\,S\,cm^{-1}$ at room temperature have been prepared. It is found that the electrolytes show excellent mechanical strength as well as good chemical and electrochemical stability. The optimum blend of PVA–PECH is 1:0.2 and this electrolyte forms a uniform and homogeneous polymer film. By contrast, PVA–PECH (1:1) exhibits phase-separation morphology. Solid-state Zn–air cells using the blended polymer electrolytes have been assembled and examined. The cells display good electrochemical characteristics. It is conducted that an alkaline PVA–PECH polymer electrolyte with a blend ratio of 1:0.2 is a potential candidate for application in alkaline batteries.

References

[1] F.M. Gray, Solid Polymer Electrolytes—Fundamental and Technological Application, VCH, New York, 1991.
[2] D.E. Fenton, J.M. Parker, P.V. Wright, Polymer 14 (1973) 589.
[3] P.V. Wright, Br. Polym. J. 7 (1975) 319.
[4] M.B. Armand, J.M. Chabagno, M.J. Duclot, in: M.J. Duclot, P. Vashishta, J.M. Mundy, G.K. Shenoy (Eds.), Fast Ion Transport in Solids, 1979.
[5] C.P. Fonseca, T.T. Cezare, S. Neves, J. Power Sources 112 (2002) 395.
[6] L. Fan, Z. Dang, C.W. Nan, M. Li, Electrochim. Acta 48 (2002) 205.
[7] H.J. Rhoo, H.T. Kim, J.K. Park, T.S. Hwang, Electrochim. Acta 42 (1997) 1571.
[8] X.D. Huang, S.H. Goh, Polymer 43 (2000) 583.
[9] S.M.D.S. Neiro, D.C. Dragunski, A.F. Rubira, Eur. Polym. J. 36 (2000) 583.
[10] C. Capiglia, P. Mustarelli, E. Quartarone, C. Tomasi, A. Magistri, Solid State Ionics 118 (1999) 73.
[11] C.J. Leo, G.V.S. Rao, B.V.R. Chowdari, Solid State Ionics 148 (2002) 159.
[12] P.A.R.D. Jayathilaka, M.A.K.L. Dissanayake, I. Albinsson, B.E. Mellander, Electrochim. Acta 47 (2002) 3257.
[13] C.C. Tambelli, A.C. Bloise, A.V. Rosario, E.C. Pereira, C.J. Magon, J.P. Donoso, Electrochim. Acta 47 (2002) 1677.
[14] C. Wang, Y. Wei, G.R. Ferment, W. Li, T. Li, Mater. Lett. 39 (1999) 206.
[15] J.F. Fauvarque, S. Gunot, N. Bouzir, E. Salmon, J.F. Penneau, Electrochim. Acta 40 (1995) 2449.
[16] S. Gunot, E. Salmon, J.F. Penneau, F. Fauvarque, Electrochim. Acta 43 (1998) 1163.
[17] N. Vassal, E. Salmon, F. Fauvarque, Electrochim. Acta 45 (2000) 1527.
[18] N. Vassal, E. Salmon, J.F. Fauvarque, J. Electrochem. Soc. 146 (1999) 20.
[19] C.C. Yang, J. Power Sources 109 (2002) 497.
[20] C.C. Yang, S.J. Lin, J. Power Sources 112 (2002) 497.
[21] C.C. Yang, S.J. Lin, Mater. Lett. 57 (2002) 873.